Strain-induced growth of SiO_2 dots by liquid phase deposition

C. W. Liu[a)]
Department of Electrical Engineering and Graduate Institute of Electronics Engineering, National Taiwan University, Taipei, Taiwan, Republic of China and Electronics Research and Service Organization, Industrial Technology Research Institute, HsinChu, Taiwan, Republic of China

B.-C. Hsu, K.-F. Chen, M. H. Lee, and C.-R. Shie
Department of Electrical Engineering and Graduate Institute of Electronics Engineering, National Taiwan University, Taipei, Taiwan, Republic of China

Pang-Shiu Chen
Electronics Research and Service Organization, Industrial Technology Research Institute, HsinChu, Taiwan, Republic of China

(Received 19 August 2002; accepted 9 December 2002)

Silicon dioxide dots are deposited on the Si cap layers of self-assembled Ge dots using a liquid phase deposition method. The Si capping layer directly above the Ge dots has a tensile strain, while the Si cap on the wetting layer is not strained. The tensile strain can enhance the silicon dioxide nucleation and deposition on Si surface, and SiO_2 dots are directly formed on the top of Ge dots with the SiO_2 wetting layers between the dots. The step height and base width of the dots increase with the deposition time. A metal-oxide-semiconductor photodetector is fabricated using the liquid-phase-deposited oxide, and has a responsivity of 0.08 mA/W at 1550 nm. © *2003 American Institute of Physics.* [DOI: 10.1063/1.1542682]

The SiGe/Si heterostructures have attracted great attention in the high-speed electronics and optoelectronics applications.[1,2] The strain engineering in the Si/Ge material system can change the band structures such as band discontinuity, effective mass, electron mobility, and the band degeneracy. Various heterojunction devices such as heterojunction bipolar transistors (HBT),[3] high electron mobility transistors,[4,5] and strained Si/Ge channel field-effect transistors (FET)[6,7] were demonstrated. Strain can also control the layer growth, and self-assembled Ge dots on Si are demonstrated with material properties and optical properties.[8,9] In this letter, we demonstrate the dot structures of silicon dioxide can be grown on Si/Ge self-assembled layers with dot density similar to the underlying Ge dot density.

To avoid material degradation such as strain relaxation and Ge outdiffusion, the low-temperature oxide is often required to reduce the thermal budget of SiGe device process. Liquid phase deposition (LPD) is a promising low-temperature process for SiO_2 formation with the advantages of low cost, selective growth, and high throughput. Based on the reaction of H_2SiF_6 with water to form hydrofluoric acid and solid SiO_2,[10,11] the oxide prepared by liquid phase deposition can be deposited on Ge or Si substrates.[12–15] The Si/Ge quantum dots are used to generate local strain on Si layers, and are prepared by ultrahigh vacuum chemical vapor deposition (UHVCVD) on *p*-type Si (001) substrates. After a Si buffer layer of 50 nm was grown, 5 or 10 periods of Ge/Si bilayers were grown to form the self-assembled Ge dots at the temperature of 600 °C under the Stranski–Krastanov (SK) growth mode.[16,17] The Ge layers are separated by 20 nm Si spacer layers. A 3 nm (nominal thickness) Si cap was deposited above the top layer of self-assembled Ge layer as the starting layer for the subsequent LPD oxide deposition. All ultrahigh vacuum chemical vapor deposition (UHVCVD) layers are *p*-type with the estimated concentration on the order of 1×10^{16} cm^{-3}. For comparison, rapid thermal oxidation (RTO) at 700 °C was also performed. During the LPD process, the silicic acid ($SiO_2:xH_2O$) was added to hydrofluosilicic acid (H_2SiF_6, 3 mol/L) at the temperature of 35 °C, and the solution was filtered to remove the undissolved silica. H_2O was then added to the saturated solution and enabled the solution to become supersaturated with silicon oxide. Both quantum dots samples and the bare Si control samples were placed into the immersing solution at 50 °C together for different growth time. These samples were then taken out from the solution and rinsed with deionized water. The oxide thickness of control Si wafer was determined by ellipsometry. The samples were characterized with atomic force microscopy (AFM), and transmission electron microscopy (TEM) on {110} cross sections of the samples.

Figure 1 shows the cross-section TEM image of the ten-period Ge dots structure with the base and the height of ~100 and ~6 nm, respectively. The Ge layers are separated by ~20 nm Si spacer layers. The Ge dots are self-assembled in a row vertically on the same position due to the spacer thickness smaller than the correlation length.[8] After 15 min LPD oxide growth, the SiO_2 dots are formed on Si cap directly above the Ge dots. Note that in the image, the central SiO_2 dot is clearly seen, while the dots on the left- and right-hand side exist, but the images are smeared. From the TEM images, the oxide dots have step height of 14 nm, and a wetting layer of 5 nm. The definition of the height is the step thickness between the oxide dot and the oxide wetting layer [the inset of Fig. 2(a)]. The wetting layer is a thin layer of bright contrast above the Si cap in the TEM micrograph. The

a)Author to whom correspondence should be addressed; electronic mail: chee@cc.ee.ntu.edu.tw

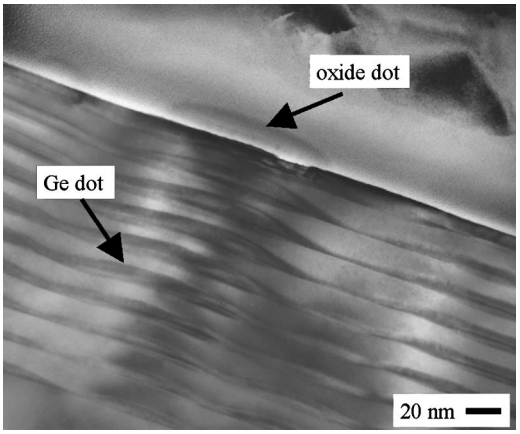

FIG. 1. Cross-section TEM micrograph of oxide dots on the self-assembled Ge quantum dots structures.

thickness (5 nm) of wetting layer obtained from TEM micrograph is similar to the oxide thickness (7 nm) on the control Si samples, measured by the ellipsometry using the refraction index of 1.458. The step height (14 nm) of oxide dots obtained from TEM is similar to AFM results (15 nm). In Fig. 2(a), the oxide dot height obtained from AFM increases with the LPD deposition time up to 27 nm. The oxide thickness on control Si is also shown in Fig. 2(a), approximately indicating the thickness of the oxide wetting layer. The base of the oxide dots also increases with deposition time from 94 (10 min) to 176 nm (25 min), as shown in Fig. 2(b). To confirm that the SiO_2 dots replicate at the sites of the Ge dots globally, AFM is performed on the five-period self-assembled Ge dots sample with a 20 nm Si spacer. The AFM image is shown in Fig. 3. The oxide dot density is $3-4\times10^9$ cm^{-2}, very similar to the Ge dot density which is measured on the samples with the same growth condition without the top Si cap. This indicates that the deposited SiO_2 dots are vertically aligned on embedded Ge dots. The mechanism of this alignment is probably related with the strain field on the Si cap. Due to the relaxation of Ge dots, the Si cap area directly on the Ge dots has tensile strain,[8] while the Si cap area above the Ge wetting layer is strain free (Fig. 4). The nucleation of oxide during LPD process may be much easier on the Si area with tensile strain than the strain-free Si area. Since the step height of oxide dots increases with deposition time faster than the oxide thickness on control Si as

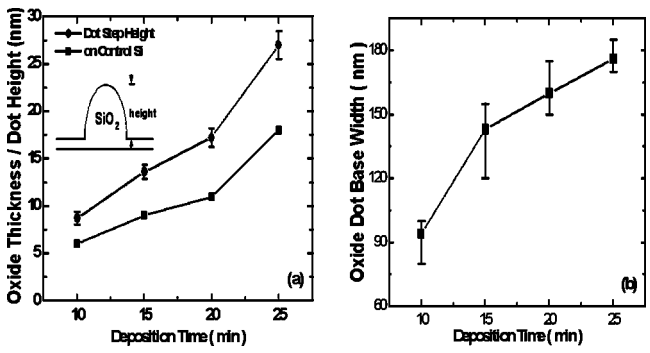

FIG. 2. (a) Step height of LPD oxide dots and the oxide thickness on the control Si wafers vs LPD growth time. The oxide thickness on the control Si wafers is similar to the wetting layer thickness; (b) Base width of oxide dots as a function of deposition time.

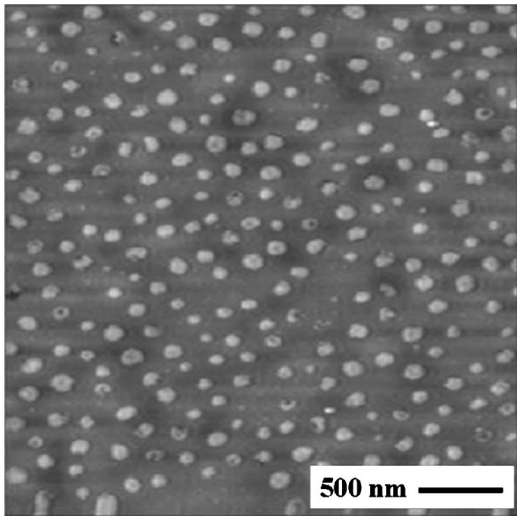

FIG. 3. AFM surface image of LPD oxide on the Si cap layer of 5-period self-assembled Ge dot sample with 20 nm Si spacers.

shown in Fig. 2(a), the tensile strain also enhances the growth rates on tensile strained areas. The strain effect can last at least for oxide dot thickness of $\sim$45 nm [sum of the oxide height and oxide thickness at the deposition time of 25 min in Fig. 2(a)], since the step height still increases at this oxide thickness.

To have a metal–oxide–semiconductor (MOS) structure, aluminum is deposited on the LPD oxide and is patterned to form a MOS photodetector[18] with a circular area of 3×10^{-4} cm^2. The infrared of 1550 nm wavelength is shined on the edge of the MOS photodetector through an optical fiber. The photogenerated minority carriers (electron) can be collected by the gate electrode under the positive gate bias by diffusion and drift (as shown in the inset). A responsivity of 0.08 mA/W (efficiency of $\sim1\times10^{-4}$) is obtained with the dark current as 0.3 mA/cm^2 from the MOS photodetector. Figure 5 is the current–voltage curves with and without light exposure.

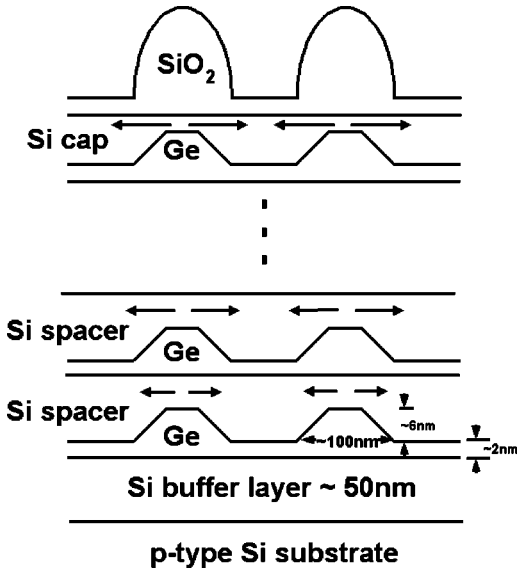

FIG. 4. Schematic diagram of strain field distribution. The Si cap area above the Ge dots has a tensile strain, and the Si cap area on Ge wetting layers is strain free.

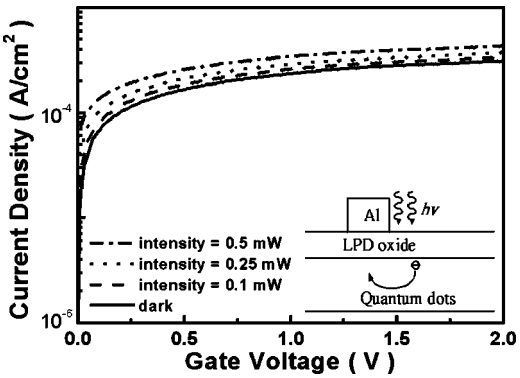

FIG. 5. Current–voltage curves of a MOS photodetector using the LPD oxide. The wavelength of infrared exposure is 1550 nm. The photogenerated carriers can be collected by lateral drift and diffusion.

In summary, the strain field on the Si cap of self-assembled quantum dots can have preferential oxide deposition during liquid phase deposition process. The oxide dots are formed on the Si cap with tensile strain, and are aligned vertically with Ge dots embedded in the Si caps. The oxide wetting layer is deposited between oxide dots on the Si cap of self-assembled Ge dots. This strain controlled deposition is demonstrated in the LPD process, similar to the epitaxial quantum dot growth reported in Si/Ge system.

This work is partially supported by National Science Council, ROC, under Contract Nos. (91-2120-E-002-007, and 91-2215-E-002-027).

[1] T. P. Pearsall, CRC Crit. Rev. Solid State Mater. Sci. **15**, 551 (1989).
[2] J. C. Bean, J. Vac. Sci. Technol. B **4**, 1427 (1986).
[3] C. A. King, J. L. Hoyt, and J. F. Gibbons, IEEE Trans. Electron Devices **36**, 2093 (1989).
[4] K. Ismail, B. S. Meyerson, S. Rishton, J. Chu, S. Nelson, and J. Noccra, IEEE Electron Device Lett. **13**, 229 (1992).
[5] J. Welser, J. L. Hoyt, and J. F. Gibbons, IEEE Electron Device Lett. **15**, 100 (1994).
[6] T. Mizuno, S. Takagi, N. Sugiyama, H. Satake, A. Kurobe, and A. Toriumi, IEEE Electron Device Lett. **21**, 230 (2000).
[7] U. Konig and F. Schaffler, IEEE Electron Device Lett. **14**, 205 (1993).
[8] O. G. Schmidt and K. Eberl, Phys. Rev. B **61**, 13721 (2000).
[9] L. Vescan, T. Stoica, O. Chretien, M. Goryll, E. Mateeva, and A. Muck, J. Appl. Phys. **87**, 7275 (2000).
[10] H. Nagayama, H. Honda, and H. Kawahara, J. Electrochem. Soc. **135**, 2013 (1988).
[11] T. Goda, H. Nagayama, A. Hishinuma, and H. Kawahara, Mater. Res. Soc. Symp. Proc. **105**, 283 (1988).
[12] B.-C. Hsu, W.-C. Hua, C.-R. Shie, K.-F. Chen, and C. W. Liu, Electrochem. Solid State Lett. (to be published).
[13] A. Hishinuma, T. Goda, and M. Kitaoka, Appl. Surf. Sci. **49**, 405 (1991).
[14] C.-F. Yeh, C.-L. Chen, and G.-H. Lin, J. Electrochem. Soc. **141**, 3177 (1994).
[15] J.-S. Chou and S.-C. Lee, Appl. Phys. Lett. **64**, 1971 (1994).
[16] T. I. Kamins, D. A. A. Ohlberg, R. S. Williams, W. Zhang, and S. Y. Chou, Appl. Phys. Lett. **74**, 1773 (1999).
[17] D. J. Eaglesham and M. Cerullo, Phys. Rev. Lett. **64**, 1943 (1990).
[18] C. W. Liu, W. T. Liu, M. H. Lee, W. S. Kuo, and B. C. Hsu, IEEE Electron Device Lett. **21**, 307 (2000).